ELSEVIER

Biochimica et Biophysica Acta 1461 (1999) 47–57

BIOCHIMICA ET BIOPHYSICA ACTA
BBA

www.elsevier.com/locate/bba

Hydration of lipoplexes commonly used in gene delivery: follow-up by laurdan fluorescence changes and quantification by differential scanning calorimetry

Danielle Hirsch-Lerner *, Yechezkel Barenholz

Laboratory of Membrane and Liposome Research, Department of Biochemistry, The Hebrew University – Hadassah Medical School, P.O. Box 12272, Jerusalem 91120, Israel

Received 14 June 1999; accepted 17 August 1999

Abstract

Lipoplexes, which are formed spontaneously between cationic liposomes and negatively charged nucleic acids, are commonly used for gene and oligonucleotide delivery in vitro and in vivo. Being assemblies, lipoplexes can be characterized by various physicochemical parameters, including size distribution, shape, physical state (lamellar, hexagonal type II and/or other phases), sign and magnitude of electrical surface potential, and level of hydration at the lipid–DNA interface. Only after all these variables will be characterized for lipoplexes with a broad spectrum of lipid compositions and DNA/cationic lipid (L^+) mole (or charge) ratios can their relevance to transfection efficiency be understood. Of all these physicochemical parameters, hydration is the most neglected, and therefore the focus of this study. Cationic liposomes composed of DOTAP without and with helper lipids (DOPC, DOPE, or cholesterol) or of DC-Chol/DOPE were complexed with pDNA (S16 human growth hormone) at various DNA^-/L^+ charge ratios (0.1–3.2). (DOTAP = *N*-(1-(2,3-dioleoyloxy)propyl)-*N,N,N*-trimethylammonium chloride; DC-Chol = (3β-[*N*-(*N′*,*N′*-dimethylaminoethane)-carbamoyl]-cholesterol; DOPC = 1,2-dioleoyl-*sn*-glycero-3-phosphocholine; DOPE = 1,2-dioleoyl-*sn*-glycero-3-phosphoethanolamine). The hydration levels of the different cationic liposomes and the DNA separately are compared with the hydration levels of the lipoplexes. Two independent approaches were applied to study hydration. First, we used a semi-quantitative approach of determining changes in the 'generalized polarization' (GP) of laurdan (6-dodecanoyl-2-dimethylaminonaphthalene). This method was recently used extensively and successfully to characterize changes of hydration at lipid–water interfaces. Laurdan excitation GP at 340 nm (GP_{340}) was found to be the most informative parameter in our studies, suggesting that changes in hydration upon lipoplex formation do not involve a major liquid-crystalline to gel transition. DC-Chol/DOPE liposomes were the 'driest' of all liposome compositions. Among DOTAP-based cationic liposomes, the order of the 'driest' to the 'wettest' composition is DOTAP/Cholesterol > DOTAP/DOPE > DOTAP/DOPC > DOTAP. The GP_{340} of lipoplexes of all lipid compositions (except those based on DC-Chol/DOPE) was higher than the GP_{340} of the cationic liposomes alone and

Abbreviations: Chol, cholesterol; DC-Chol, 3β-[*N*-(*N′*,*N′*-dimethylaminoethane)-carbamoyl]-cholesterol; DMTAP, *N*-(1-(2,3-dimyristoyl)propyl)-*N,N,N*-trimethylammonium chloride; DNA^-/L^+, mole charge ratio of DNA negatively charged phosphate to positively charged lipid; DOPC, 1,2-dioleoyl-*sn*-glycero-3-phosphocholine; DOPE, 1,2-dioleoyl-*sn*-glycero-3-phosphoethanolamine; DOTAP, *N*-(1-(2,3-dioleoyloxy)propyl)-*N,N,N*-trimethylammonium chloride; DPH, 1,6-diphenylhexa-1,3,5-triene; DSC, differential scanning calorimetry; Hepes, *N*-(2-hydroxyethyl)piperazine-*N′*-(2-ethanesulfonic acid); L^+, positively charged lipid; laurdan, 6-dodecanoyl-2-dimethylaminonaphthalene; LUV, large (≥100 nm) unilamellar vesicles; MLV, multilamellar vesicles; PC, phosphatidylcholine; PCS, photon correlation spectroscopy; PE, phosphatidylethanolamine; TMADPH, 1-(4-trimethylammoniumphenyl)-6-phenyl-1,3,5-hexatriene

* Corresponding author. Fax: +972-2-641-1663; E-mail: danieleh@pob.huji.ac.il or yb@cc.huji.ac.il

PII: S0005-2736(99)00145-5

increased with increasing DNA^-/L^+ charge ratio, reaching a plateau at a charge ratio of 1.0, suggesting an increase in dehydration at the lipid–water interface with increasing DNA^-/L^+ charge ratio. Confirmation was obtained from the second method, differential scanning calorimetry (DSC). DOTAP/DOPE lipoplexes with charge ratio 0.44 had 16.5% dehydration and with charge ratio 1.5, 46.4% dehydration. For DOTAP/Chol lipoplexes with these charge ratios, there was 17.9% and 49% dehydration, respectively. These data are in good agreement with the laurdan data described above. They suggest that the dehydration occurs during lipoplex formation and that this is a prerequisite for the intimate contact between cationic lipids and DNA.

Keywords: Hydration; Laurdan; Differential scanning calorimetry; Cationic lipid; DNA

1. Introduction

Lipoplexes are complexes of cationic lipids (with or without helper lipids) with nucleic acids. The electrostatic interactions between the positively charged liposomes and the negatively charged nucleic acids result in spontaneous formation of lipoplexes [1]. Prior to complexation, both liposome and DNA surfaces are highly hydrated. Lipoplex formation involves removal of water molecules as the hydrated surface of the lipid assembly and the DNA come into close contact [2]. In the liposomes, the water provides the driving force in the formation of the lipid bilayer [3], while water molecules bound to the headgroup region play a major role in membrane stabilization (i.e., by preventing fusion) and controlling lipid–lipid interactions, as exemplified by lowering gel to liquid-crystalline phase transition temperature [4,5]. Water is also an integral part of nucleic acid structure; it interacts with the nucleic acids and is mainly responsible for the stabilization of its secondary and tertiary structure [6]. For the β helix, 20 water molecules are bound per nucleotide [6,7]. The water molecules of the primary shell (about ten molecules) interact directly with phosphates, sugar oxygens, and with the polar groups of the bases that are within reach in the DNA structure [8,9].

There has been little investigation of the changes in hydration level of lipids and DNA as a result of lipoplex formation. This study aims to fill this gap by using two independent methods; one is based on the generalized polarization (GP) of the fluorophore laurdan (6-dodecanoyl-2-dimethylaminonaphthalene) [10,11] used in the present work to follow the interfacial water changes in the cationic liposomes upon their complexation with DNA. Laurdan is located at the hydrophilic-hydrophobic interface of the bilayer [12], with the lauric acid part aligned parallel to the phospholipid acyl chain regions, and its fluorescent naphthalene residue located at the level of the glycerol backbone [13]. The fluorescence properties of laurdan are notably sensitive to the polarity of the environment [12] and to the dynamics of the environment. Laurdan was used to compare hydration level of cationic liposomes based on DOTAP alone, DOTAP/DOPE, DOTAP/Chol, and DC-Chol/DOPE and of lipoplexes formed upon interaction of these liposomes with plasmid DNA at a DNA/cationic lipid ratio range from 0.1 to 3.2.

The second method is differential scanning calorimetry (DSC), which has been used before to determine hydration of lipid vesicles [14,15] and of DNA [6]. Here, we used DSC to determine levels of tightly bound water of the cationic liposomes, DNA, and the lipoplexes formed at a DNA/cationic lipid ratio of 0.44 and 1.5.

Both methods show that, indeed, lipoplex formation involves dehydration.

2. Materials and methods

2.1. DNA preparation

Escherichia coli containing the plasmid S16 hGH was kindly given by Dr. O. Meyuhas of our department [16]. The plasmid size was 4.8 kbp. The plasmid S16 hGH was grown and isolated using a QIAGEN Mega Plasmid kit (QIAGEN, Hilden, Germany). After plasmid purification, DNA was dissolved in 20 mM Hepes (pH 7.4) and 10 mM NaCl (unless stated otherwise) and its concentration was quantified by organic phosphate determination [17]. Agarose gel (1%) electrophoresis showed that the plasmid DNA was mostly ($>70\%$) in a supercoiled form, free from chromosomal DNA or RNA. In the different

DNA batches the ratio of absorbance at 260 nm to that at 280 nm was about 1.8–1.9, indicating lack of contamination with proteins [18].

2.2. Liposome preparation

DOTAP (*N*-(1-(2,3-dioleoyloxy)propyl)-*N,N,N*-trimethylammonium chloride), DOPE (1,2-dioleoyl-*sn*-glycero-3-phosphoethanolamine), and DOPC (1,2-dioleoyl-*sn*-glycero-3-phosphocholine) were obtained from Avanti Polar Lipids (Alabaster, AL). Cholesterol (purity of 99%) was purchased from Sigma (St. Louis, MO) and DC-Chol (3β-[*N*-(*N′,N′*-dimethylaminoethane)-carbamoyl]-cholesterol) was a gift from Dr. L. Huang (Department of Pharmacology and Pharmaceutical Sciences, University of Pittsburgh, PA). Laurdan was purchased from Lambda (Graz, Austria). All other chemicals were of analytical grade.

Fluorescent-labeled large unilamellar vesicles (LUV) were prepared by mixing *tert*-butyl alcohol solutions of the different lipids with laurdan in *N*,*N*-dimethylformamide at a ratio of 1000 moles of lipid per mole of fluorophore. The mixture was freeze-dried overnight, and the LUV were prepared as described in [19]. The particle size distribution of the liposome dispersions was determined by photon correlation spectroscopy (PCS) using a Coulter N4SD (Coulter Electronics, Hialeah, FL) [17]. LUV of all compositions have unimodal size distribution of similar mean size ($\sim 100 \pm 20$ nm).

2.3. Fluorescence measurements

An aliquot of laurdan-labeled liposomes was diluted with 1 ml of 20 mM Hepes buffer (pH 7.4) to the desired concentration. The cationic lipid concentration was 0.39 mM in the range of $DNA^-/L^+ < 1$ and 0.039 mM at $DNA^-/L^+ > 1$. Fluorescence measurements were performed on a Perkin–Elmer LS 50B luminescence spectrometer using a 1 cm light path cell. Bandpasses of the monochromators were 5 nm and 10 nm at $DNA^-/L^+ < 1$ and $DNA^-/L^+ > 1$, respectively. Temperature was maintained at 25°C with a water-circulating bath. Fluorescence intensities were measured 5 min after addition of DNA. All data were corrected for light scattering, as described by Borenstain and Barenholz [20].

Laurdan was used to follow changes in hydration level of lipid vesicles by Gratton and coworker [11]. In solvents of high polarity, laurdan shifts its emission spectrum to higher wavelengths due to dipolar relaxation processes [12]. When associated with phospholipids, laurdan excitation and emission spectra depend strongly on the phase state of the lipid. This shift is related to differences in level of hydration between the gel and liquid-crystalline phases. A 50-nm red shift is observed in laurdan emission by moving from the gel to the liquid-crystalline phase, as maximum emission shifts from 440 nm to 490 nm [11]. This shift is defined by a steady-state fluorescence parameter called generalized polarization (GP) which quantitatively connects these spectral changes by considering the relative fluorescence intensities of the blue and red edge regions of the emission and excitation spectra, respectively [11,12].

The excitation GP value was calculated as follows:

$$\text{Excitation GP} = (I_{440} - I_{490})/(I_{440} + I_{490}),$$

where I_{440} and I_{490} are the intensities of the emission at wavelengths of 440 nm and of 490 nm [11] at the excitation wavelengths of 340 nm (excitation GP_{340}) or 410 nm (excitation GP_{410}), respectively.

The emission GP value was calculated as follows:

$$\text{Emission GP} = (I_{410} - I_{340})/(I_{410} + I_{340}),$$

where I_{340} and I_{410} are the intensities of the excitation at wavelengths of 340 nm and of 410 nm at the emission wavelengths of 440 nm (emission GP_{440}) or 490 nm (emission GP_{490}). The choice of the emission and the excitation wavelengths for the calculations of GP values was based on the characteristic emission and excitation wavelengths of pure gel and liquid-crystalline phases [21].

Laurdan GP spectra in phospholipid vesicles allow quantification of the two coexisting phases, gel and liquid-crystalline. In addition, it was found that the GP value was independent of the pH (in the range 4–10) and the type of polar headgroup [12]. Therefore, the process of dipolar relaxation which sets the spectral properties must be related to the number of water molecules around the fluorescent moiety of laurdan [12]. Their studies using phospholipid vesicles demonstrated that laurdan is sensitive to the dynamics as well as to the polarity of the surrounding membrane.

2.4. Differential scanning calorimetry (DSC) measurements

DSC was used to quantify the amount of tightly bound water per mole total lipid (H_2O/L), mole DNA phosphate (H_2O/DNA), or mole lipid plus DNA in lipoplex (H_2O/lipoplex), as explained below. The details of the method are described elsewhere [22]. The samples of lipids (or lipid mixtures), DNA, or lipoplexes were lyophilized to constant weight. A weighed amount of water was added which was always less than the amount of lipids or DNA or lipoplexes. The sample in the sealed crucible was scanned from −30°C to 30°C using the Mettler TA4000 differential scanning calorimeter until reproducible thermograms were obtained (usually two or three times). Scanning was at the rate of 2°C/min. No loss of weight occurred during the scans. Calculation of bound water is based on ice–water fusion heat enthalpy of 325 J/g obtained from a calibration curve, in agreement with published data [23]. The expected hydration values of lipoplexes were calculated from the known compositions of lipoplexes for $DNA^-/L^+ = 0.44$ and $DNA^-/L^+ = 1.5$. For the specific hydration levels of both MLV and DNA at $DNA^-/L^+ = 0.44$, we used $H_2O/L^+ + (H_2O/DNA \times 0.22)$ = calculated bound water of lipoplex, while at $DNA^-/L^+ = 1.5$, we used $H_2O/L^+ + (H_2O/DNA \times 0.75)$ = calculated bound water of lipoplex. The factors of 0.22 and 0.75 are related to the ratio of moles DNA phosphate to moles total lipids, the latter being twice the moles of cationic lipid. When there was an overlap the heat enthalpy of the lipid phase transition was subtracted from the ice–water fusion heat enthalpy for the specific hydration calculations of the lipoplexes. The difference between calculated and measured hydration of lipoplexes was used to calculate the change in level of hydration due to lipoplex formation.

3. Results

3.1. Laurdan fluorescence measurements

The laurdan results given below are described as GP_{340} because the excitation at 340 nm proved to be the most sensitive to the effect of DNA when compared with the excitation GP spectrum at 410 nm (which was almost unaffected by DNA) and the emission GP spectra (data not shown). This suggests that the changes in hydration measured here are not due to changes in lipid phase but related directly to hydration variations around the laurdan fluorophore (see Discussion).

Table 1
Laurdan GP at the excitation of 340 nm (GP_{340}) of the LUV of different lipid compositions without DNA at the two lipid concentrations used in the experiment

Lipid	GP_{340} at 0.78 mM lipid	GP_{340} at 0.08 mM lipid
DOTAP	−0.27 ± 0.008	−0.29 ± 0.056
DOTAP/DOPE	−0.07 ± 0.015	−0.08 ± 0.05
DOTAP/DOPC	−0.12 ± 0.016	−0.19 ± 0.036
DOTAP/Chol	0.28 ± 0.005	0.32 ± 0.047
DC-Chol/DOPE	0.513	0.43 ± 0.043
DOPE/DOPC	0.028	0.03 ± 0.001
DOPC	−0.11 ± 0.004	NA

The excitation GP at $\lambda = 340$ nm of the various cationic liposome compositions is presented in Table 1. This value expresses the hydration level of the lipid bilayer in the absence of DNA. The GP_{340} values for the LUV are in the order DC-Chol/DOPE > DOTAP/Chol ≫ DOPC/DOPE > DOTAP/DOPE > DOTAP. That is, DC-Chol/DOPE is the least hydrated, and DOTAP the most hydrated.

The effect of DNA on GP_{340} for various cationic LUV is described as $\Delta GP_{340} = GP_{340}$ of lipoplexes $- GP_{340}$ of liposomes. Fig. 1 shows that for most liposome compositions used there is a continuous increase in ΔGP_{340} with increasing DNA to cationic lipid mole ratio. The largest effect on ΔGP_{340} was observed with DOTAP/DOPE LUV. Among the DOTAP-containing liposomes, DNA causes the smallest increase in ΔGP_{340} of 100% DOTAP/DOPC LUV. For DC-Chol/DOPE LUV, $\Delta GP_{340} \approx 0$. The GP_{340} of the uncharged DOPC/DOPE liposomes remained constant and unaffected upon addition of DNA. At $DNA^-/L^+ > 1$, the effect of DNA on ΔGP_{340} reaches a plateau (see Table 2).

The effect of NaCl on DNA–(DOTAP/DOPE 1/1) complex formation was evaluated (Fig. 2). The GP value of DOTAP/DOPE liposomes without DNA in 20 mM Hepes was −0.045, while in the presence of 150 mM NaCl the value rises to −0.03, indicating a

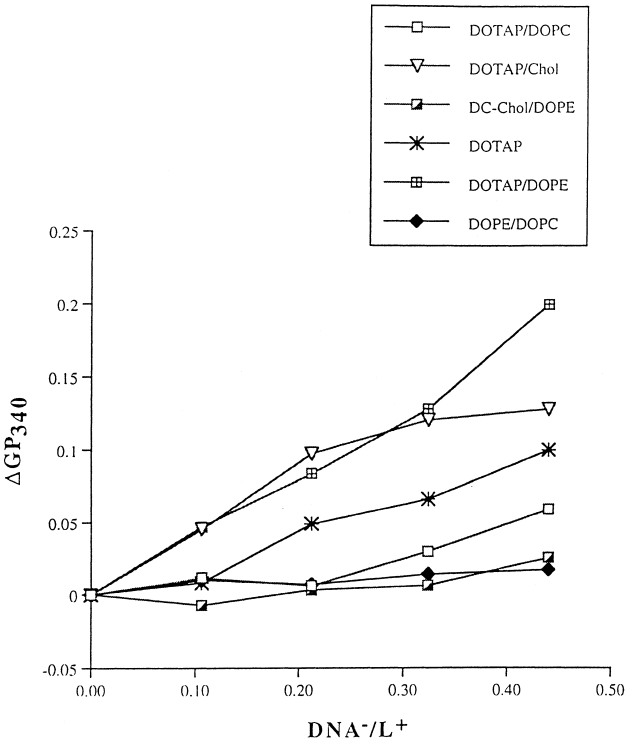

Fig. 1. Effect of mole ratio DNA to cationic lipid ($DNA^-/L^+ < 0.5$) on ΔGP_{340} for lipoplexes containing various lipids. Noncationic LUV composed of DOPC/DOPE were used as control. $\Delta GP_{340} = GP_{340}$ of lipoplexes $- GP_{340}$ of liposomes. For GP_{340} of liposomes see Table 1.

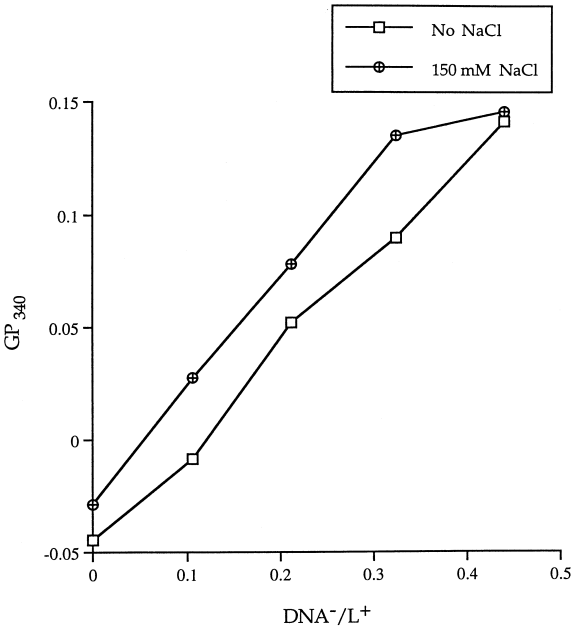

Fig. 2. Effect of 150 mM NaCl on laurdan GP_{340} of DOTAP/DOPE (1/1) LUV at ratios of $DNA^-/L^+ < 0.5$.

small salt-induced dehydration at the lipid–water interface. The effect of 150 mM NaCl on the lipoplex (up to $DNA^-/L^+ = 0.5$) was additive to the effect of DNA on the lipid hydration. On the other hand, for lipoplexes of $DNA^-/L^+ > 1$, GP_{340} in the presence of 150 mM was constant, i.e., was not affected by the addition of DNA (data not shown).

3.2. DSC measurements

The thermograms of the lipid dispersions alone are presented in Fig. 3. The T_m of DOPE is −16°C and of DOPC in the range of −14 to −22°C, as reviewed in [24]. The T_m of DOTAP is −11.9°C [19]. One can clearly see the endothermic peak of the water around 0°C (peak 2 in Fig. 3, thermograms a,b,c,e,f,g).

The inset in Fig. 3 compares the endothermic peaks of H_2O and D_2O, showing a shift of ~6°C with D_2O. When DOTAP/DOPC MLV were prepared in the presence of D_2O the endothermic peak of the water (peak 2) shifted to ~3°C (thermogram d). The thermogram of DOTAP/Chol MLV (thermogram e) did not display peak 1 (the lipid endotherm) but only the peak 2 of water. This result is expected since 50 mol% cholesterol abolishes completely phase transition of lipids [25,26], shifting the lipid bilayer to a liquid ordered phase [27,28].

On the other hand, thermograms of DNA without an excess of water (a and b in Fig. 4) do not show the endothermic peak of the water around 0°C, but a very much broader peak between −28°C and −10°C.

Table 2
Laurdan ΔGP_{340} of lipoplexes composed of different lipid compositions at $DNA^-/L^+ \geq 1$

Ratio DNA^-/L^+	ΔGP_{340}				
	DOTAP	DOTAP/DOPE	DOTAP/DOPC	DOTAP/Chol	DC-Chol/DOPE
1	0.092	0.1	0.067	0.093	0.007
3.15	0.099	0.11	0.091	0.117	−0.008

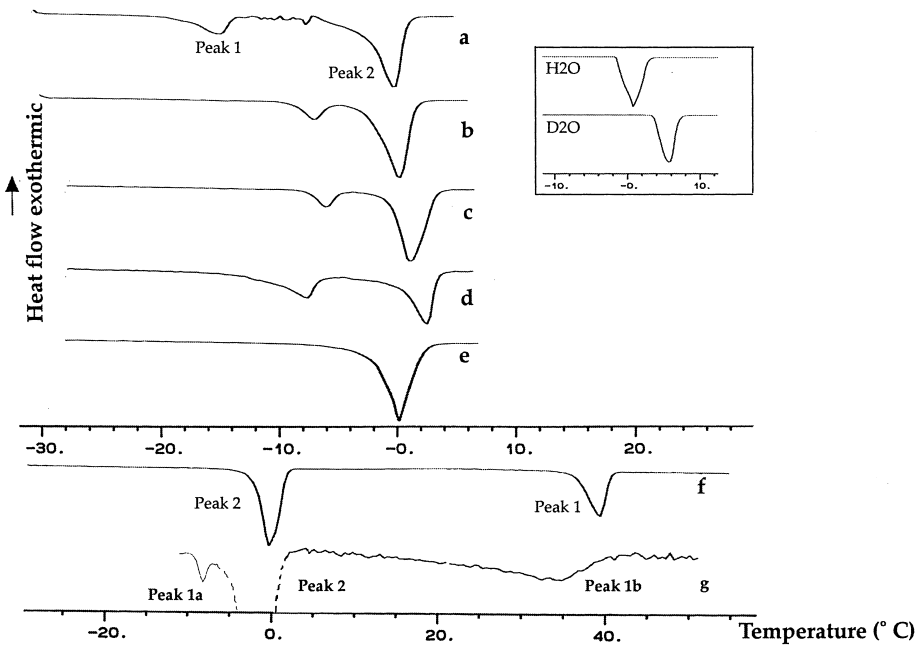

Fig. 3. Thermograms of cationic liposomes (MLV). (a) DOTAP in H_2O; (b) DOTAP/DOPE (mole ratio 1:1) in H_2O; (c) DOTAP/DOPC (mole ratio 1:1) in H_2O; (d) DOTAP/DOPC (mole ratio 1:1) in D_2O; (e) DOTAP/Chol (mole ratio 1:1) in H_2O; (f) DMTAP in H_2O; (g) DMTAP/DOPE in H_2O. Peak 1 is the endotherm of gel-to-liquid-crystalline main lipid phase transition and peak 2, the endotherm of the melting of free water. Sensitivity is 0.5 mW for thermogram g, 2 mW for thermograms a,d,f, and 5 mW for b,c,e. Inset: thermograms of pure H_2O and D_2O.

This indicates that all the water molecules in the sample are tightly bound to the DNA. Curve c in Fig. 4 shows that when an excess of unbound water is present in the DNA solutions, it undergoes ice–water transition at ca. −1°C.

The thermograms of the lipoplexes based on DOTAP/DOPE and DOTAP/Chol liposomes are presented in Fig. 5. In all the samples the endothermic peak of the water was shifted to lower temperatures (around −3°C and −4°C). The thermogram of the lipoplexes based on DOTAP/DOPE liposomes at $DNA^-/L^+ = 0.44$ (thermogram a) shows, in addition to the peak of water, a peak that corresponds to the free DOTAP/DOPE which is in excess at this ratio. As mentioned above, when the helper lipid DOPE was replaced by Chol, the phase transition of the DOTAP was cancelled (thermogram c). At $DNA^-/L^+ = 1.5$, the thermograms of the DOTAP/DOPE and the DOTAP/Chol lipoplexes (thermograms b and d) exhibit the broad peak of the water as seen in Fig. 4.

From the thermograms of the plasmid DNA it was calculated [22] that there are 12 moles of water tightly bound per mole phosphate of plasmid DNA, which is in a good agreement with the value of 10 moles (in the first shell) previously reported [8]. Fourteen moles of bound water per mole lipid were found for DOTAP/DOPE liposomes and 11 moles for DOTAP/Chol liposomes (Table 3). These data are in good agreement with the laurdan GP_{340} data

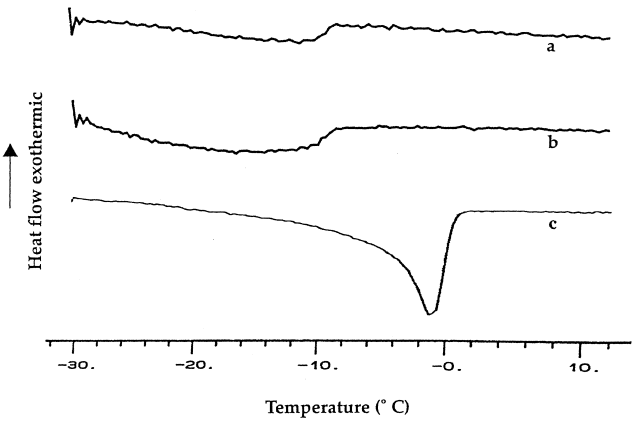

Fig. 4. Thermograms of plasmid DNA without and with excess of water. (a) 0.76 mg of DNA with 0.68 mg of water. (b) 1.62 mg with 1.36 mg of water. Sensitivity for a and b is 2 mW. (c) 0.95 mg DNA with an excess of water (1.31 mg). Sensitivity is 1 mW.

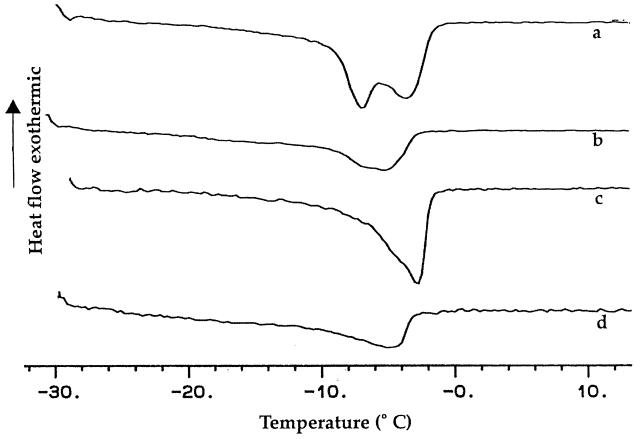

Fig. 5. Thermograms of lipoplexes composed of DOTAP/DOPE and DNA at $DNA^-/L^+ = 0.44$ (a) and at $DNA^-/L^+ = 1.5$ (b), and of DOTAP/Chol at $DNA^-/L^+ = 0.44$ (c) and at $DNA^-/L^+ = 1.5$ (d). Sensitivity is 2 mW.

which suggest that DOTAP/Chol liposomes are less hydrated than DOTAP/DOPE LUV (Table 1). Therefore, the theoretical number of bound water molecules in the case of $DNA^-/L^+ = 0.44$ with DOPE as a helper lipid is expected to be 16.9 per lipoplex containing 1 mole lipid plus 0.44 mole DNA phosphates, while at the ratio of $DNA^-/L^+ = 1.5$ the expected value is 23.32 moles of bound water per lipoplex containing 1 mole lipid plus 1.5 mole DNA phosphates (see Section 2 for the calculations) (Table 3). In the other lipoplex composition, using cholesterol as a helper lipid, 13.6 moles of bound water per lipoplex were calculated at the ratio of $DNA^-/L^+ = 0.44$, while at the ratio of $DNA^-/L^+ = 1.5$, 20 moles of bound water per lipoplex were calculated (see Table 3). Table 3 shows clearly that the lipoplexes of (DOTAP/DOPE)/DNA and (DOTAP/Chol)/DNA are less hydrated than the LUV and the DNA before they form lipoplexes. The level of dehydration increases with increase in DNA^-/L^+ ratio. This is in good agreement with the laurdan results described in Fig. 1.

Controls composed of DOPE/DOPC liposomes were studied; the number of moles of bound water per mole lipid without DNA was the same as with DNA in both ranges of DNA^-/L^+ (data not shown). DMTAP/DOPE liposomes were also used as an additional control; for this MLV, one can observe a phase separation between a DOPE-rich phase with a T_m of −8°C (Fig. 3, peak 1a in thermogram g) and a DMTAP-rich phase having a broad asymmetric endotherm with a T_m of 26°C (Fig. 3, peak 1b in thermogram g) while DMTAP gel-to-liquid-crystalline phase transition of DMTAP MLV occurred at a higher temperature, ∼40°C (Fig. 3 peak 1 in thermogram f), and therefore the lipid phase transition of DMTAP/DOPE does not overlap the water endotherm (Fig. 3, peak 2 in thermogram g). The DMTAP-rich phase is a broad and asymmetric peak, and its enthalpy (ΔH) is one-fifth that of DMTAP alone. The endotherms of both DOPE and DMTAP are distinguished from the H_2O endotherm (thermogram g in Fig. 3). Eight moles of bound water per mole lipid were calculated for DMTAP/DOPE liposomes. This value is lower than the 14 moles of water for liposomes composed of DOTAP/DOPE. The DMTAP molecule is less hydrated than DOTAP, probably because DMTAP, being a saturated lipid [29], having a $T_m > 37$°C is at 37°C in the solid-ordered phase which is drier than the liquid-disordered phase of DOTAP. A dehydration of 30% was measured when DMTAP/DOPE liposomes were complexed with DNA at $DNA^-/L^+ = 1.5$, which is lower than the dehydration of

Table 3
Dehydration during lipoplex formation determined from the difference between calculated and measured specific hydration: DSC study using DOTAP/DOPE (1/1) and DOTAP/Chol (1/1) liposomes

LUV composition	LUV-specific bound water (mol H_2O/mol lipid)	Lipoplex-specific bound water (mol H_2O/mol (DNA phosphate+lipid))					
		$DNA^-/L^+ = 0.44$			$DNA^-/L^+ = 1.5$		
		expected	observed	% change	expected	observed	% change
DOTAP/DOPE (1/1)	14	16.9	14.12 ± 0.12	−16.5	23.32	12.50 ± 0.85	−46.4
DOTAP/Chol (1/1)	11	13.6	11.17 ± 0.81	−17.9	20	10.17 ± 1.45	−49

Hydration of DNA determined by DSC shows 12 moles of bound water per mole DNA phosphate. For more details see Section 2.

the equivalent lipoplex in which DOTAP is the cationic lipid (Table 3).

4. Discussion

Lipoplexes formed spontaneously upon interaction of DNA with cationic liposomes at a mole ratio of 0.1–3.2 were investigated using laurdan generalized polarization (GP) and DSC. The laurdan GP value depends mainly on changes of hydration of the bilayer headgroup region either due to changes in the ratio between the less hydrated gel (solid-ordered) phase and the more hydrated liquid-crystalline (liquid-disordered) phase or due to other reasons, but not due to the type of bilayer headgroup charge [11]. Therefore, the spectral properties of laurdan must be due to the level of water located at the hydrophobic–hydrophilic interface of the bilayer where the fluorescent laurdan is anchored [12].

The use of laurdan GP at various wavelengths enables one to distinguish between changes in hydration related to phase change or others reasons [11]. Laurdan GP was used previously to demonstrate that cholesterol induces dehydration of lipid bilayers [30,31]. The excitation GP at 410 nm selects the gel phase, while the excitation GP at 340 nm selects all the lipid phases equally (Gratton, personal communication). Differences in GP values of the various liposomes used for lipoplex formation, as well as changes in GP due to the formation of lipoplexes, are related to changes in the excitation at 340 nm and not at 410 nm (emission), suggesting that the changes in hydration level are not related to changes in lipid phase.

The hydration level of the cationic liposomes alone (Table 1) was measured through the laurdan probe and showed, as expected, that lipid compositions containing cholesterol were less hydrated (higher GP) [30] than liposomes of other lipid compositions. The large difference in GP_{340} between the vesicles containing and those lacking DC-Chol or cholesterol and those containing or lacking ester phospholipids as helper lipids are related to the difference in their physical state. The cholesterol- or DC-Chol-containing vesicles are at the less hydrated liquid-ordered phase, while the system lacking the cholesterol nucleus is in the liquid-disordered phase [27,28]. This is clearly demonstrated by our DSC data (compare Fig. 3e to Fig. 3a–c).

The lower hydration observed with DOTAP liposomes formulated with either DOPE or DOPC than for 100% DOTAP liposomes can be explained as follows: the quaternary amine of DOTAP could interact with the phosphate group of the phospholipids DOPE or DOPC, forming a salt bridge (or ion pair) [32]; such a bond will reduce the possibilities of hydrogen bonding of water with the charged groups. Moreover, DOTAP/DOPC liposomes were found to be more hydrated than DOTAP/DOPE liposomes. This difference is expected since lamellar PC dispersions bind more water and more tightly than do PE-enriched dispersions [33].

Laurdan GP_{340} of cationic lipoplexes compared to those of the cationic liposomes showed a general trend of dehydration over all the DNA^-/L^+ range. As shown by the increase in ΔGP_{340}, most of the dehydration occurred at $DNA^-/L^+ < 0.5$, reaching a plateau above one (Fig. 1 and Table 2). This is in accord with our previous observations on the neutralization of cationic lipids by DNA in the lipoplexes followed by the fluorescent probe 4-heptadecyl-7-hydroxycoumarin (HC), which also showed a plateau in maximal percent neutralization at $DNA^-/L^+ > 1$ (Fig. 4 in [1]). In addition, other studies had shown that the DNA/cationic lipid ratio of 1.0 is a critical ratio [34,35]. Gershon et al. [31] found that above the cationic lipid/DNA mole ratio of about 1, two processes took place: DNA-induced lipid fusion and liposome-induced DNA collapse. When DNA is added to DC-Chol/DOPE liposomes, there is no increase in GP_{340} (Fig. 1). This may be related to the fact that the lipid of these liposomes is less hydrated than that of others used in this study (Table 1).

At this range of $DNA^-/L^+ > 1$, DNA being in excess, most charges of the cationic lipids in the lipoplex are neutralized by the negative charges of the DNA phosphates. Comparing liposomes composed of DOTAP and various helper lipids, laurdan GP shows the greatest dehydration for the lipoplexes composed of DOTAP/DOPE; DOPE 'helps' to enhance dehydration. One possible mechanism is that DOPE enables the DNA to come closer to the interface due to the salt formation between the DOPE phosphate and the DOTAP quaternary amine [32].

The dehydration of both DNA and the lipids is a requirement to obtain a tight contact during their interaction [1,36]. This tight association was visualized by video microscopy with fluorescently labeled DNA and lipids [37]. The effect of DNA on the electrical surface potential determined through the use of HC indicates that the distance between the DNA phosphate and the HC fluorophore (located at the same plane as the quaternary amine of DOTAP) is shorter than 0.8 nm [1].

A previous study [19] demonstrated changes in the exposure of the upper part of the lipid acyl chains to water upon DNA–lipid complexation. The liposomes were fluorescently probed with TMADPH, the quaternary amine of which is located at the lipid–water interface. Dehydration in the upper part of the lipid acyl chain region was obtained in lipoplexes composed of $DNA^-/L^+ = 1.0$, while increased hydration in this region was found when DNA^-/L^+ of lipoplexes was $= 0.6$ [19]. While the results obtained with laurdan (this paper) agree with those obtained with TMADPH [19] for $DNA^-/L^+ = 1.0$, they show opposite trends at $DNA^-/L^+ = 0.6$, i.e., partial dehydration versus increased exposure to water for laurdan and TMADPH, respectively.

How can this discrepancy be explained? The two fluorophores are located at different planes of the lipid bilayer: the naphthalene of laurdan is found at the glycerol backbone plane, while the diphenylhexatriene moiety of TMADPH is located parallel to the upper part of the acyl chain, occupying almost 50% of the acyl chain length. At high DNA^-/L^+ ratios, there is almost a complete cationic lipid neutralization [1] and this interaction induces a homogeneous lipid condensation without phase separation or membrane defects. This condensation involves removal of a fraction of the water molecules both tightly and loosely bound to the lipid headgroup which are available to affect TMADPH in the upper part of the acyl chains. The DSC study at $DNA^-/L^+ = 0.44$ shows that the dehydration was a third of that at $DNA^-/L^+ = 1.5$ (Table 3). In parallel, there is a partial and less than expected neutralization of cationic lipids [1]. Also, the DNA induces lipid phase separation between condensed domains in which the lipid interacts with DNA and non-condensed DNA-free lipid domains [19]. It seems that there is a qualitative agreement between level of cationic lipid neutralization and lipid dehydration. It is possible that the dehydration occurs only at the lipid domains in which DNA interacts with the cationic lipid. Therefore, the water molecules present at DNA-free lipid domains (or continuum) are available to interact with the TMADPH and, due to the membrane defects, more water molecules find their way to interact with the TMADPH in the lipid upper acyl chain region.

The laurdan GP approach is mainly qualitative in nature and gives trends of changes in level of hydration. Also a more quantitative and direct approach is determination of the level of tightly bound water by DSC. First, we used DMTAP ($T_m = 40°C$; Fig. 3, peak 1 in thermogram f) and DMTAP/DOPE (thermogram g in Fig. 3) and distinguished between endotherms related to lipid gel-to-liquid-crystalline phase transition and those of water-to-ice-water transition (Fig. 3, peak 2 in f,g). For the DOTAP/DOPC system, we added another control to distinguish between gel-to-liquid-crystalline phase transition and water-to-ice-water transition. By replacing H_2O with D_2O, peak 1 (lipid) and peak 2 (water) were shifted to higher temperatures (see Fig. 3, thermograms c,d and inset): peak 2 shifted to a larger extent than peak 1. A third proof of the identification of peak 1 as the lipid endotherm and peak 2 as the water endotherm derives from Fig. 3, where on thermogram e (DOTAP/Cholesterol 1/1), peak 1 completely disappeared due to the known effect of cholesterol of abolishing the gel-to-liquid phase transition [24,25]. Thus, the contribution of hydration and the gel-to-liquid-crystalline phase transition to the thermograms can be distinguished, and therefore DSC can be used to quantify lipid, DNA, and lipoplex hydration.

A significant dehydration (over 40%) was observed in both formulations (DOTAP/DOPE and DOTAP/Chol) at the charge ratio DNA^-/L^+ of 1.5 (Table 3). During this complex formation, the DNA secondary structure is changed from a B-type helix (high activity of water) to a C-type helix and even to a Ψ^--type (partial condensed tertiary structure) [38]. The DNA, as a condensation consequence, becomes more bent and/or flexible. Our own circular dichroism (CD) study ([39] and Simberg and Barenholz, unpublished results) showed a partial transition from B-to-C-type DNA with appearance of Ψ^- tertiary structure at

$DNA^-/L^+ = 0.6$ in the presence of DOPE or cholesterol. It is known that a complete $B \rightarrow C$ transition is coupled with a large DNA dehydration [40]. Therefore, the CD data suggest also that DNA–cationic lipid interactions are accompanied by partial dehydration of the DNA, in addition to charge neutralization by the cationic lipids. DNA condensation occurs when about 90% of the negatively charged phosphates of DNA are neutralized [39]. The CD measurements identify the secondary and tertiary structures of DNA, while DSC indicates both DNA and lipid dehydration. Although we do not yet have direct information on DNA neutralization, we can estimate from binding isotherms that at $DNA^-/L^+ = 0.5$, 85–90% of the DNA is complexed to DOTAP/Chol and 98% of the DNA is complexed to DOTAP/DOPE; therefore DNA should be condensed (Even-Chen and Barenholz, unpublished results). The fact that the dehydration of DOTAP/Chol is shown much better by DSC than by the laurdan GP_{340} (compare Fig. 1 and Table 3) suggests that laurdan monitors mainly the changes in the lipid hydration and is less sensitive to changes in hydration of the DNA in the lipoplex, while DSC shows the overall dehydration.

Physiological saline (150 mM NaCl) did not impede lipoplex formation in the DNA^-/L^+ ratio < 1 (see Fig. 2) and > 1. Similar results were monitored through the use of TMADPH [19] or HC fluorophore (Hirsch-Lerner et al., unpublished results) in DOTAP/DOPE-based lipoplexes in the presence of 150 mM NaCl. Moreover, at $DNA^-/L^+ = 0.5$ the lipoplex dispersion in the presence of 150 mM NaCl contained little free DNA, as determined by agarose electrophoresis (Even-Chen and Barenholz, unpublished results). NaCl (150 mM) by itself induced a partial dehydration; the effect of DNA on the hydration was additive (Fig. 2). These results are in agreement with the findings that fusion between cationic liposomes and anionic liposomes was not disturbed by NaCl up to 150 mM [41].

Cationic lipids facilitating polar domain dehydration and hydrophobic domain destabilization displayed the highest levels of transfection [29]. This high transfection activity may be due to a better ability of the lipoplexes to be taken up and processed inside the cells by fusing with the endosome membrane, thereby escaping lysosomal degradation [29]. Therefore, nonbilayer lipid structures might play a direct role in transfection via fusion or membrane destabilization of target cells [42]. So far, only a few studies [43,44] have focused on structural DNA modifications as a result of complexation with cationic liposomes. The degree of supercoiling, which is affected by dehydration [41], may also be a prominent factor in various biological mechanisms involving DNA, such as transcription and replication, as well as transfection [42]. Further investigations will be carried out on changes in DNA upon lipoplex formation.

Acknowledgements

This study was supported by Israel Science Foundation Grant 8004/98 to Y.B. We would like to thank Dr. L. Huang of the Department of Pharmacology and Pharmaceutical Sciences, University of Pittsburgh, Pittsburgh, PA and Dr. P.L. Felgner of Vical, San Diego, CA, for their gifts of DC-Chol and DMRIE/DOPE (1/1), respectively, and Dr. O. Meyuhas of our department for the S16 hGH plasmid. Mr. S. Geller is acknowledged for help in editing the manuscript.

References

[1] N.J. Zuidam, Y. Barenholz, Biochim. Biophys. Acta 1368 (1998) 115–128.
[2] J. Israelachvili, H. Wennerström, Nature 379 (1996) 219–225.
[3] J.M. Boggs, Biochim. Biophys. Acta 906 (1987) 353–404.
[4] V. Luzzati, F. Husson, J Cell. Biol. 12 (1962) 207–219.
[5] H. Hauser, in: F. Franks (Ed.), Lipids in Water: A Comprehensive Treatise, vol. 4, Plenum Press, New York, 1975, pp. 209–304.
[6] D. Eagland, in: F. Franks (Ed.), Nucleic acids, Peptides and Proteins in Water: A Comprehensive Treatise, vol. 4, Plenum Press, New York, 1975, pp. 305–518.
[7] W. Saenger, in: Principles of Nucleic Acids Structure, Springer, New York, 1983, Chapter 17.
[8] M. Kochoyan, J.L. Leroy, Curr. Opin. Struct. Biol. 5 (1995) 329–333.
[9] B. Schneider, K. Patel, H.M. Berman, Biophys. J. 75 (1998) 2422–2434.
[10] T. Parasassi, A.M. Giusti, E. Gratton, E. Monaco, M. Raimondi, G. Ravagnan, O. Sapora, Int. J. Radiat. Biol. 65 (1994) 329–334.

[11] T. Parasassi, E. Gratton, J. Fluoresc. 5 (1995) 59–69.
[12] T. Parasassi, G. De Stasio, G. Ravagnan, R.M. Rush, E. Gratton, Biophys. J. 60 (1991) 179–189.
[13] M. Viard, J. Gallay, M. Vincent, O. Meyer, B. Robert, M. Paternostre, Biophys. J. 73 (1997) 2221–2234.
[14] D. Bach, B. Sela, I.R. Miller, Chem. Phys. Lipids 31 (1982) 381–394.
[15] A.S. Ulrich, M. Sami, A. Watts, Biochim. Biophys. Acta 1191 (1994) 225–230.
[16] S. Levy, D. Avni, N. Hariharan, R.P. Perry, O. Meyuhas, Proc. Natl. Acad. Sci. USA 88 (1991) 3319–3323.
[17] Y. Barenholz, S. Amselem, in: G. Gregoriadis (Ed.), Liposome Technology, 2nd ed., vol. 1, CRC Press, Boca Raton, FL, 1993, pp. 527–616.
[18] T. Maniatis, E.F. Fritsch, J. Sambrook, Molecular Cloning. A Laboratory Manual, Cold Spring Harbor Laboratory, Cold Spring Harbor, New York, USA, 1982.
[19] D. Hirsch-Lerner, Y. Barenholz, Biochim. Biophys. Acta 1370 (1998) 17–30.
[20] V. Borenstain, Y. Barenholz, Chem. Phys. Lipids 64 (1993) 117–127.
[21] T. Parasassi, G. De Stasio, A. d'Ubaldo, E. Gratton, Biophys. J. 57 (1990) 1179–1186.
[22] Y. Barenholz, E. Freire, T.E. Thompson, M.C. Correa-Freire, D. Bach, I.R. Miller, Biochemistry 22 (1983) 3497–3501.
[23] O. Tirosh, R. Kohen, J. Katzhendler, R. Gorodetsky, Y. Barenholz, J. Chem. Soc., Perkin Trans. 2 (1997) 383–389.
[24] D. Marsh, Handbook of Lipid Bilayers, CRC Press, Boca Raton, FL, 1990.
[25] B.D. Ladbroke, R.M. Williams, D. Chapman, Biochim. Biophys. Acta 150 (1968) 333–340.
[26] R.L. Biltonen, D. Lichtenberg, Chem. Phys. Lipids 64 (1993) 129–142.
[27] O.G. Mouritsen, K. Jorgensen, Chem. Phys. Lipids 73 (1994) 3–25.
[28] J.H. Ipsen, G. Karlström, O.G. Mouritsen, H. Wennerström, M.J. Zuckermann, Biochim. Biophys. Acta 905 (1987) 162–172.
[29] M.J. Bennett, A.M. Aberle, R.P. Balasubramaniam, J.G. Malone, R.W. Malone, M.H. Nantz, J. Med. Chem. 40 (1997) 4069–4078.
[30] T. Parasassi, M. Di Stefano, M. Loiero, G. Ravagnan, E. Gratton, Biophys. J. 66 (1994) 763–768.
[31] T. Parasassi, M. Di Stefano, M. Loiero, G. Ravagnan, E. Gratton, Biophys. J. 66 (1994) 120–132.
[32] N.J. Zuidam, Y. Barenholz, Biochim. Biophys. Acta 1329 (1997) 211–222.
[33] E.G. Finer, A. Darke, Chem. Phys. Lipids 12 (1974) 1–16.
[34] H. Gershon, R. Ghirlando, S.B. Guttman, A. Minsky, Biochemistry 32 (1993) 7143–7151.
[35] S.J. Eastman, C. Siegel, J. Tousignant, A.E. Smith, R.K. Cheng, R.K. Scheule, Biochim. Biophys. Acta 1325 (1997) 41–62.
[36] J.O. Radler, I. Koltover, T. Salditt, C.R. Safinya, Science 275 (1997) 810–814.
[37] I. Koltover, T. Salditt, J.O. Rädler, C.R. Safinya, Science 281 (1998) 78–81.
[38] V.A. Bloomfield, Biopolymers 44 (1997) 269–282.
[39] N.J. Zuidam, D. Hirsch-Lerner, S. Margulies, Y. Barenholz, Biophys. Acta 1419 (1999) 207–220.
[40] B. Wolf, S. Hanlon, Biochemistry 14 (1975) 1661–1670.
[41] C.-H. Lee, H. Mizvsawa, T. Kakefuda, Proc. Natl. Acad. Sci. USA 78 (1981) 2838–2842.
[42] H. Weintraub, P.F. Cheng, K. Conrad, Cell 46 (1986) 115–122.
[43] T. Akao, T. Fukumoto, H. Ihara, A. Ito, FEBS Lett. 391 (1996) 215–218.
[44] K.W.C. Mok, P.R. Cullis, Biophys. J. 73 (1997) 2534–2545.